

BELLCOMM, INC.

TR-68-720-1

DETERMINATION OF ORBITS OF PLANETARY  
ARTIFICIAL SATELLITES AND PLANETARY  
GRAVITATIONAL FIELDS

May 24, 1968

C. L. Greer  
C. C. H. Tang

Work performed for Manned Space Flight, National Aeronautics and  
Space Administration under Contract NASW-417.

BELLCOMM, INC.

TABLE OF CONTENTS

	ABSTRACT
I.	INTRODUCTION
II.	FORMULATION OF MATHEMATICAL MODEL
III.	OBSERVED AND KNOWN QUANTITIES
IV.	SOLUTION OF THE NONLINEAR EQUATIONS
	A. CLASSICAL DIFFERENTIAL CORRECTION METHOD
	B. NEWTON RAPHSON METHOD
	C. GENERALIZED NEWTON RAPHSON METHOD
	D. GENERALIZED DIFFERENTIAL CORRECTION METHOD
V.	SIMULATION COMPARISON
	A. STATIONARY PLANET
	B. MOVING PLANET
VI.	GENERAL STATISTICAL ESTIMATION CRITERION
VII.	PERTURBATIONS DUE TO AN OBLATE PLANET
VIII.	CONCLUSIONS
	APPENDIX I
	APPENDIX II
	REFERENCES

BELLCOMM, INC.

ABSTRACT

The state-vector of a planetary artificial satellite is determined by using Earth-based range-rate measurements. The satellite velocity component in the direction from the planet-center to Earth-center instead of that from the satellite to an observation station is computed in a theoretical model. The relatively simple least squares estimation criterion thus obtained for the case of a planet at infinite distance facilitates the comparison study of numerical methods of solving a system of non-linear equations.

Simulation results obtained by programming in double precision show that the longitude of the ascending node of a planetary satellite can be determined to prescribed accuracy within a few days of tracking.

The comparison study is made among (1) classical differential correction method, (2) Newton-Raphson method, (3) generalized differential correction method, and (4) generalized Newton-Raphson method. It indicates that the new generalized differential correction method has a convergence range of initial estimate wider than the other methods. The extension in the convergence range of initial estimate enhances the success of obtaining a preliminary state-vector in a short tracking period and is particularly important in planetary missions.

The effects of perturbations of non-central forces on the satellite can be incorporated in the formulation without resorting to numerical integration.

# BELLCOMM, INC.

## DETERMINATION OF ORBITS OF PLANETARY ARTIFICIAL SATELLITES AND PLANETARY GRAVITATIONAL FIELDS

### I. INTRODUCTION

Orbit determination is considered to mean, for a prescribed mathematical model, the statistical estimation of a trajectory from noisy observation data. In principle, the general methods of orbit determination and gravitational field deduction are analogous whether the spacecraft to be tracked is a terrestrial, lunar, planetary, or solar satellite. However, the availability of observational data is strongly dependent on the particular tracking geometry involved, and the determination of a planetary satellite orbit is inherently more complicated than that of a terrestrial or lunar satellite orbit. For example, the preliminary state-vector of an Earth satellite can be approximately established by a number of observation stations, each located at a different latitude and making range-rate measurements or a combination of range and angular measurements in a relatively short tracking interval, say a few revolutions of the Earth satellite. The situation is quite different for Earth-based tracking of a lunar or planetary satellite. Existing tracking facilities are capable of measuring angular position with an optimistic one-sigma uncertainty of  $0.01^\circ$ , which corresponds to about 65 km and 12,000 km, respectively, at the lunar distance and at Mars distances during oppositions. Accordingly, at such large distances the uncertainty of angular measurements is not compatible with the conservative one-sigma uncertainties of  $10^{-4}$  m/sec (S-band at 60-second sample rate) for range-rate and 10 m (light-second) for range.

Because of the slow relative "rotational" motion between the Earth and another planet, the orientation plane of a planetary satellite as viewed from an observation station on the Earth does not change very much within a few revolutions of a planetary satellite. Viewing from stations located at different sites on the Earth does not improve the "resolution" because the angular separation is negligible. In fact this is why the spectroscopic binary star technique fails to yield information on the longitude of the ascending node. To circumvent the difficulty, the tracking interval must be extended so that data points are spaced far enough apart in time and in position to ensure significant uncorrelated measurements. An alternative is to place another observation station far from the Earth station.

In this paper the planetary satellite velocity component in the direction from the center of the planet to the center of the Earth instead of that in the conventional direction from the satellite to an observation station on the Earth is computed in a mathematical model. The least squares estimation criterion obtained this way is relatively simple for the case of a planet assumed at infinite distance from the Earth. This simplification facilitates comparison studies of numerical methods of solving a system of highly nonlinear equations. For the actual case of finite distance between the Earth and a planet, the least squares estimation criterion thus obtained is slightly different from that of the conventional approach. Its implications are discussed in Section VI.

The classical differential correction method of orbit determination requires an initial state-vector estimate sufficiently close to the desired solution that the iterative

process of differential correction will converge to the solution. The constraint on the initial estimate in the classical differential correction method is a consequence of linearization of the highly nonlinear dynamical equations of motion of the spacecraft. For terrestrial or lunar satellite orbit determination, the present model of the Earth-Moon system and our present tracking capability are accurate enough to supply an initial state-vector estimate within the convergence range of the classical differential correction process. However, because of imperfect mathematical models of the planetary systems, uncertainties in physical constants, and possible malfunction in the final orbit injection mechanism, initial estimates of the state-vector for a planetary satellite may not be within the range of convergence. Accordingly, it is desirable to devise a different or complementary orbit determination program that has a wider convergence range of initial estimate than the classical differential correction method. The orbit determination program presented herein is an attempt in that direction. Comparison studies indicate that the new numerical method of solving a system of nonlinear equations indeed widens the convergence range of initial estimate.

Simulation results show that the state-vector of a planetary satellite can be determined to prescribed accuracy within a few days of tracking. The effects of perturbations of non-central forces on the satellite can be incorporated in the formulation without resorting to numerical integration.

The paper is intended to present a self-contained study of the orbit determination of an artificial satellite.

II. FORMULATION OF MATHEMATICAL MODEL

Consider a unit sphere with center P at the center of a planet. Let  $\underline{r}$  and  $\dot{\underline{r}}$  be, respectively, the instantaneous radius vector and velocity vector of a satellite relative to the dynamical center P of the planet. Let the orthogonal right handed coordinate system XYZ with its origin at P be the non-rotating "inertial" reference selected at an initial time of tracking  $t_0$ . At  $t = t_0$  the Y-axis is chosen to lie in the orbital plane of the planet, the -Z-axis to point at the center of the Earth, and the X-axis to be the principal axis pointing in a northerly direction as shown in Figure 1. A second orthogonal coordinate system  $x'y'z'$  with its origin at P is attached to the rotating line connecting the centers of the planet and the Earth so that at  $t = t_0$  the two coordinate systems coincide. The plane  $x'y'$  is the so-called plane-of-the-sky which is always perpendicular to the line joining the centers of the Earth and the planet.

With respect to the "inertial" plane XY (the plane-of-the-sky at  $t = t_0$ ) the orientation of the orbital plane is uniquely defined as shown in Figure 1 by the longitude of the ascending node  $\Omega$ , the inclination  $i$ , and the argument of periplanet  $\omega$ . The ranges of these three angular elements are:

$$0 \leq \Omega \leq 2\pi \quad ; \quad 0 \leq i \leq \pi \quad ; \quad 0 \leq \omega \leq 2\pi \quad .$$

The satellite velocity component in the direction of the planet-Earth line can be expressed in terms of those angles. Let  $\underline{r}$ , the radius vector of the satellite with respect to the planet be represented as:

$$\underline{r} = r \hat{\underline{r}} \quad , \quad (1)$$

where  $r$  is the magnitude of the radius vector  $\underline{r}$ , and  
 $\hat{\underline{r}}$  is the unit vector in the direction of  $\underline{r}$ .

The velocity vector therefore is:

$$\dot{\underline{r}} = \dot{r} \hat{\underline{r}} + r \dot{f} \hat{\underline{r}}_{\perp} = \|\dot{\underline{r}}\| \angle \phi, \quad (2)$$

where  $\dot{f}$  is the rate of change of the true anomaly  $f$ ,  
 $\hat{\underline{r}}_{\perp}$  is the unit vector perpendicular to the radius  
vector  $\underline{r}$  and is in the direction of motion,  
 $\|\dot{\underline{r}}\|$  is the Euclidean norm of  $\dot{\underline{r}}$ , and  
 $\phi$  is the angle between  $\underline{r}$  and  $\dot{\underline{r}}$ .

It can be shown that for a Keplerian orbit

$$\dot{r} = \left[ \frac{\mu}{a(1-e^2)} \right]^{1/2} e \sin f, \quad (3)$$

and

$$r\dot{f} = \left[ \frac{\mu}{a(1-e^2)} \right]^{1/2} (1+e \cos f), \quad (4)$$

where  $a$  is the semi-major axis of the satellite orbit,  
 $e$  is the eccentricity of the orbital ellipse, and  
 $\mu$  is the gravitational parameter.



Accordingly, equation (2) takes the form

$$\dot{\underline{r}} = \left[ \frac{\mu(1+2e \cos f + e^2)}{a(1-e^2)} \right]^{1/2} \frac{1}{\tan^{-1} \left( \frac{1+e \cos f}{e \sin f} \right)} \cdot \quad (5)$$

The components of the velocity vector  $\dot{\underline{r}}$  in the "inertial" frame XYZ at  $t = t_0$  are:

$$\begin{aligned} \dot{\underline{r}} \cdot \hat{\underline{X}} &= \|\dot{\underline{r}}\| [\cos \Omega \cos(\omega + f + \phi) - \sin \Omega \sin(\omega + f + \phi) \cos i] \quad , \\ \dot{\underline{r}} \cdot \hat{\underline{Y}} &= \|\dot{\underline{r}}\| [\sin \Omega \cos(\omega + f + \phi) + \cos \Omega \sin(\omega + f + \phi) \cos i] \quad , \\ \dot{\underline{r}} \cdot \hat{\underline{Z}} &= \|\dot{\underline{r}}\| \sin(\omega + f + \phi) \sin i \quad . \end{aligned} \quad (6)$$

When  $t > t_0$ , the orientation of the Earth relative to the planet changes in such a way that, using the  $-Z$ -axis and the  $YZ$ -plane as references, the  $-z'$ -axis points toward the center of the Earth in a direction defined by the planetocentric right ascension  $\alpha$  and declination  $\delta$ . The values of  $\alpha$  and  $\delta$  can be computed from the relative motions of the Earth and planet with the aid of the ephemerides. The corresponding orientation change of the  $x'y'$ -plane due to that of the  $-z'$ -axis can be obtained from the following trigonometric relations in terms of Euler angles  $\Omega'$ ,  $i'$ , and  $\omega'$  with respect to the  $XY$ -plane:

$$i' = \cos^{-1}(\cos \alpha \cos \delta) \quad , \quad (7)$$

$$\Omega' = \sin^{-1} \frac{\sin \delta}{\sin i'} \quad . \quad (8)$$

For vanishing declination  $\delta$ ,  $\Omega'$  vanishes and the inclination  $i'$  is equal to the right-ascension, as they should. In general,  $i'$ ,  $\Omega'$ , or  $\alpha$ ,  $\delta$  are functions of time. (Fig. 1 shows the case corresponding to  $\Omega' = 0$ .)

The transformation matrix  $N$  that converts the quantities in the XYZ frame into the  $x'y'z'$  frame is:

$$N = \begin{bmatrix} \cos\Omega' \cos\omega' - \sin\Omega' \sin\omega' \cos i' & \sin\Omega' \cos\omega' + \cos\Omega' \sin\omega' \cos i' & \sin\omega' \sin i' \\ -\cos\Omega' \sin\omega' - \sin\Omega' \cos\omega' \cos i' & -\sin\Omega' \sin\omega' + \cos\Omega' \cos\omega' \cos i' & \cos\omega' \sin i' \\ \sin\Omega' \sin i' & -\cos\Omega' \sin i' & \cos i' \end{bmatrix} \quad (9)$$

The component of the satellite velocity in the direction of the  $-z'$ -axis is the radial velocity and is represented by:

$$\begin{aligned} \dot{\underline{r}} \cdot (-\hat{\underline{z}}') &= - \left[ \frac{\mu(1+2e \cos f + e^2)}{a(1-e^2)} \right]^{1/2} \left\{ (\sin i \cos i' - \cos \Omega \cos i \sin i' \cos \Omega' \right. \\ &\quad \left. - \sin \Omega \cos i \sin i' \sin \Omega') \sin(\omega + f + \phi) \right. \\ &\quad \left. + (\cos \Omega \sin i' \sin \Omega' - \sin \Omega \sin i' \cos \Omega') \cos(\omega + f + \phi) \right\}. \end{aligned} \quad (10)$$

The components normal to  $\hat{\underline{z}}'$  can also be obtained. By eliminating  $\phi$ , equation (10) takes the form:

$$\begin{aligned}
\dot{\underline{r}} \cdot (-\hat{\underline{z}}') = & - \left[ \frac{\mu}{a(1-e^2)} \right]^{1/2} \left\{ [\sin i \cos i' \right. \\
& - (\cos \Omega \cos \Omega' + \sin \Omega \sin \Omega') \cos i \sin i'] [\cos(\omega+f) + e \cos \omega] \\
& \left. + [(\sin \Omega \cos \Omega' - \cos \Omega \sin \Omega') \sin i'] [\sin(\omega+f) + e \sin \omega] \right\} = H.
\end{aligned}
\tag{11}$$

For convenience we let the right side of equation (11) be designated as H, the computed value of the velocity component in the  $-z'$  direction, and the left side, the corresponding observed value. For  $i' = 0$  and  $\Omega' = 0$ , equation (11) reduces exactly to the solution of the classical spectroscopic binary star technique [1]:

$$\dot{\underline{r}} \cdot (-\hat{\underline{z}}') = - \left[ \frac{\mu}{a(1-e^2)} \right]^{1/2} \sin i [\cos(\omega+f) + e \cos \omega] \quad . \tag{12}$$

With sufficient observational data in Doppler form, estimates of the state-vector ( $a, e, \tau, \Omega, i, \omega$ ) and the planet gravitational parameter  $\mu$  can be obtained from equation (11) with the aid of Kepler's equation

$$m = \left( \frac{\mu}{a^3} \right)^{1/2} (t - \tau) = \sin^{-1} \left[ \frac{(1-e^2)^{1/2} \sin f}{1+e \cos f} \right] - e \left[ \frac{(1-e^2)^{1/2} \sin f}{1+e \cos f} \right]. \tag{13}$$

where  $m$  is the mean anomaly and  $\tau$  is the time of periplanet passage. It is seen that the gravitational parameter  $\mu$  is an integral part of parameter estimation processes in equation (11).

### III. OBSERVED AND KNOWN QUANTITIES

Equation (11) as it stands is valid only for observations taken at the center of a non-rotating Earth, which is assumed at an infinite distance from a planet. In actual situations, however, observation stations are on the surface of the rotating Earth, which is at a variable finite distance from a planet. To take account of these effects, equation (11) has to be generalized.

In Figure 2, points  $S_0$ , E, and P are, respectively, the centers of the Sun, Earth, and planet. S is the position of a planetary satellite and O is the position of the observer on the surface of the Earth. Vectorially the planetary satellite radius vector  $\underline{r}$  can be expressed as:

$$\underline{r} = \underline{D} + \underline{R} + \underline{\rho} \quad , \quad (14)$$

where  $\underline{D}$  is the vector between the centers of the Earth and the planet,

$\underline{R}$  is the vector between the center of the Earth and the observer at O, and

$\underline{\rho}$  is the vector between the satellite S and the observer at O.

The component of  $\dot{\underline{r}}$  in the planet-Earth direction can be decomposed as

$$\dot{\underline{r}} \cdot (-\hat{\underline{z}}') = (-\dot{\underline{D}} \cdot \hat{\underline{z}}' - \dot{\underline{R}} \cdot \hat{\underline{z}}' - \dot{\underline{\rho}} \cdot \hat{\underline{z}}') \quad . \quad (15)$$

For general cases the three terms on the right side of equation (15) can be obtained separately. The terms  $\dot{\underline{R}} \cdot \hat{\underline{z}}$  and  $\dot{\underline{D}} \cdot \hat{\underline{z}}$  are known quantities.  $\dot{\underline{R}} \cdot \hat{\underline{z}}$  is due to the diurnal motion of the Earth observer along the Earth-planet line and can be calculated, using data of known accuracy. The distance  $\underline{D}$  between the Earth and planet is known only in terms of the astronomical unit, which has an uncertainty in terms of absolute distance. The magnitude of the term  $\dot{\underline{D}}$  can be calculated as below from the vector relations in Figure 2

$$\underline{D} = \underline{l}_E - \underline{l}_P = q(\text{a.u.})\hat{\underline{l}}_E - s(\text{a.u.})\hat{\underline{l}}_P \quad . \quad (16)$$

where  $\underline{l}_E$  and  $\underline{l}_P$  are, respectively, the vectors between the centers of the Sun  $S_0$  and the earth E and between the centers of the Sun and the planet P,  
 $\hat{\underline{l}}_E$  and  $\hat{\underline{l}}_P$  are, respectively, the unit vectors in the direction of  $\underline{l}_E$  and  $\underline{l}_P$ , and  
 $q$  and  $s$  are, respectively, the distances in a.u. from the sun to the Earth and to the planet.

Taking the time derivative of equation (16), we have

$$\dot{\underline{D}} = (\text{a.u.})(\dot{q}\hat{\underline{l}}_E + q\dot{\theta}_E\hat{\underline{l}}_{E_{\perp}} - \dot{s}\hat{\underline{l}}_P - s\dot{\theta}_P\hat{\underline{l}}_{P_{\perp}}) \quad . \quad (17)$$

where  $\theta_P$  and  $\theta_E$ , generally not in the same plane, are, respectively, the angles between the vernal equinox  $\gamma$  and  $\underline{l}_P$  and  $\underline{l}_E$ , and

$\hat{\underline{l}}_P$  and  $\hat{\underline{l}}_E$  are, respectively, the unit vectors perpendicular to  $\underline{l}_P$  and  $\underline{l}_E$  and in the directions of motion of the planet and the Earth.

The term  $\dot{\underline{D}} \cdot \hat{\underline{z}}'$  then is

$$\begin{aligned} \dot{\underline{D}} \cdot \hat{\underline{z}}' = (\text{a.u.}) & \left[ \dot{q} \cos(\hat{\underline{l}}_E, \hat{\underline{z}}') - q \dot{\theta}_E \sin(\hat{\underline{l}}_E, \hat{\underline{z}}') \right. \\ & \left. - \dot{s} \cos(\hat{\underline{l}}_P, \hat{\underline{z}}') + s \dot{\theta}_P \sin(\hat{\underline{l}}_P, \hat{\underline{z}}') \right]. \quad (18) \end{aligned}$$

All the quantities within the bracket of equation (18) can be obtained from the ephemerides.

In tracking a planetary satellite from the Earth, the periodic Doppler shift curve with zero crossings (at instances when the satellite velocity vector is perpendicular to the  $\underline{z}'$ -axis) will have maximum amplitude when its orbit is viewed edgewise ( $i$  near  $\frac{\pi}{2}$ ) and approach vanishing amplitude when viewed transversely ( $i$  near zero). On the other hand,  $\dot{\underline{D}} \cdot \hat{\underline{z}}'$  is the same whether the orbit is viewed edgewise or transversely. The implication is that the observational data from orbits viewed edgewise are affected much less by the uncertainty in a.u. than those viewed transversely. From this point of view we can conveniently consider the uncertainty in a.u. as a biased noise which can be removed by curve fitting processes after acquisition of sufficient data.

The third term  $\dot{\underline{p}} \cdot \hat{\underline{z}}'$  in equation (15) is the quantity to be observed and can be decomposed by letting

$$\underline{\rho} = \rho \hat{\underline{\rho}} \quad , \quad \text{then} \quad \dot{\underline{\rho}} = \dot{\rho} \hat{\underline{\rho}} + \rho \dot{\theta}_{\underline{\rho}} \hat{\underline{\rho}}_{\perp} \quad , \quad (19)$$

where  $\dot{\rho}$  and  $\rho$  are, respectively, the observed range-rate and range between the observer and the satellite,  $\hat{\underline{\rho}}_{\perp}$  is the unit vector perpendicular to  $\underline{\rho}$  and is in the direction of motion, and  $\dot{\theta}_{\underline{\rho}}$  is the rate at which  $\underline{\rho}$  changes its direction.

Taking the component of  $\dot{\underline{\rho}}$  in the planet-Earth direction yields:

$$-\dot{\underline{\rho}} \cdot \hat{\underline{z}}' = -\dot{\rho} \hat{\underline{\rho}} \cdot \hat{\underline{z}}' - \rho \dot{\theta}_{\underline{\rho}} \hat{\underline{\rho}}_{\perp} \cdot \hat{\underline{z}}' = -\dot{\rho} \cos(\hat{\underline{\rho}}, \hat{\underline{z}}') - \rho \dot{\theta}_{\underline{\rho}} \sin(\hat{\underline{\rho}}, \hat{\underline{z}}') \quad . \quad (20)$$

Equation (20) indicates that complete evaluation of the term  $\dot{\underline{\rho}} \cdot \hat{\underline{z}}'$  for a finite Earth-planet requires three simultaneous measurements: (a) range-rate, (b) range, and (c) angular position of the satellite. For an infinite Earth-planet distance equation (20) can be evaluated by range-rate measurements alone. For these two special cases the state-vector and  $\mu$  can be determined from equations (11) and (13) with relative ease by any curve fitting procedure, say, the weighted least squares method for an over-determined system. For simplicity in carrying out simulations and comparison studies among methods of solution of a system of nonlinear equations, the case of infinite distance will be used in Sections IV and V.

For general cases of practical interest the distance is always finite, although large, and measurements involving only range-rate are preferred. Then equation (20) appears in a mixed form of a measured quantity and quantities which are functions of the state-vector to be estimated. The mixed form does not present any difficulty for statistical estimation of the state-vector. The estimation criterion for general cases of mixed form in equation (20) will be developed and simulations described in Section VI.

To avoid unknown refraction effects of the planetary atmosphere and ionosphere only those observational data which do not involve atmospheric and ionospheric penetration should be used.

#### IV. SOLUTIONS OF THE NONLINEAR EQUATIONS

The solution of the system of transcendental equations (11) and (13) requires a minimum of seven simultaneous measurements of range-rate to determine seven unknowns. For an overdetermined system, methods such as the weighted least squares are appropriate and can yield a more accurate estimate of the solution. Analytic methods for the solution of such a highly nonlinear system of equations are usually very difficult, therefore, numerical methods suitable for digital computers are of interest.

The estimation criterion described here is the weighted least squares method that yields a "best fit" to minimize the residuals in the measurements. Thus, the state-vector (including  $\mu$  from here on) that minimizes the weighted sum of the squares of the differences between the measurements and corresponding computed theoretical values constitutes the solution to the orbit determination problem in a statistical sense. Suppose a sequence of measurements  $M_1, M_2, M_3, \dots, M_n$  is given. For compactness this sequence will be represented by the column vector  $M$  and the state-vector  $(a, e, \tau, \Omega, i, \omega, \mu)$ , by the column vector variable  $X$ . The computed values  $H_1, H_2, H_3, \dots, H_n$  corresponding to  $M$  will be denoted by the column vector  $H(X)$ . The covariance matrix of  $M$  is given by

$$W = E \left\{ [M - E\{M\}] [M - E\{M\}]^T \right\} . \quad (21)$$



where  $E\{M\}$  means the expected value of  $M$  and  $T$  stands for transposition. For uncorrelated measurement errors in  $M$ ,  $W$  is a diagonal matrix. The quadratic form to be minimized is the scalar function

$$Q = [M-H(X)]^T W^{-1} [M-H(X)] \quad . \quad (22)$$

where  $[M-H(X)]$  is the so-called residuals in measurements and  $W^{-1}$  the weighting matrix. Under the assumption that the components of  $M$  obey a joint  $n$ -dimensional normal distribution with covariance matrix  $W$ , the value of  $X$  that minimizes equation (22) is the maximum likelihood estimate of the true value of the parameters. Now, for the nonlinear function  $H(X)$  the quadratic form  $Q$  is an extreme with respect to  $X$  if the vector function

$$F(X) = \left[ \frac{\partial H(X)}{\partial X} \right]^T W^{-1} [M-H(X)] = 0 \quad . \quad (23)$$

where  $\left[ \frac{\partial H(X)}{\partial X} \right]$  is a rectangular Jacobian matrix.

The state-vector  $X$  that (i) satisfies equation (23), (ii) renders  $\frac{\partial F}{\partial X}$  a positive definite, and (iii) yields the absolute minimum  $Q$  in equation (22), is the desired solution. In fact (iii) is the necessary and sufficient condition for the desired solution. To search for the desired solution by numerical methods, there are two possible mathematical approaches:

1. to solve the vector function  $F(X) = 0$  of equation (23) and
2. to minimize the scalar function  $Q(X)$  of equation (22) directly.

The following methods A, B, and C use the first approach and method D uses the second approach.

A. Classical Differential Correction Method

A first order Taylor series expansion of  $H(X)$  about an initial estimate  $X_0$  yields

$$H(X) = H(X_0) + \frac{\partial H(X_0)}{\partial X} [X - X_0] \quad . \quad (24)$$

Substitution of equation (24) into equation (23) gives the classical differential correction formula suitable for iteration as

$$X = X_0 + [J^T W^{-1} J]^{-1} F(X_0) \quad , \quad (25)$$

where  $J$  is a rectangular matrix symbolized by

$$J = \frac{\partial H(X_0)}{\partial X} \quad . \quad (26)$$

Solution of equation (25) exists only when the so-called normal matrix  $[J^T W^{-1} J]$  is non-singular.

The covariance matrix of errors in  $X$  in this case is

$$\epsilon = E \left\{ [J^T W^{-1} J]^{-1} F(X_0) F^T(X_0) [J^T (W^{-1})^T J]^{-1} \right\} \quad . \quad (27)$$

The square roots of the diagonal elements of  $\epsilon$  yield the associated mean error of each component of the state-vector. Also, the matrix  $\epsilon$  can be normalized to yield the correlations between the components by dividing the off-diagonal elements by the square root of the product of the corresponding diagonal elements.

The differential correction method requires an initial estimate  $X_0$  sufficiently close to the desired solution that the iterative procedure will converge to the solution. The constraint on the initial estimate is a consequence of the linearization of the highly nonlinear dynamical equations of motion.

#### B. Newton-Raphson Method

Following the Newton-Raphson method of unity dimension, we have the solution in linear predictor form for the multi-dimensional case of equation (23) as

$$X = X_0 - \left[ \frac{\partial F(X_0)}{\partial X} \right]^{-1} F(X_0) \quad (28)$$

For one-dimensional cases the error in the  $(n+1)^{th}$  approximation to the solution is proportional to the square of the error in the  $n^{th}$  approximation, and if the initial estimate is sufficiently close to the true solution, convergence is assured. A similar discussion of the convergence property for the multi-dimensional equation (28) is fairly involved but is covered in any standard numerical analysis text.

The explicit form of the Jacobian matrix  $\frac{\partial F}{\partial X}$  can be obtained by differentiating equation (23) and is

$$\frac{\partial F}{\partial X} = - \left\{ \left( \frac{\partial H}{\partial X} \right)^T W^{-1} \left( \frac{\partial H}{\partial X} \right) + \left[ W^{-1} (M-H)^D \frac{\partial}{\partial X} \right]^T \left( \frac{\partial H}{\partial X} \right) \right\}, \quad (29)$$

where  $(M-H)^D$  represents the  $n \times n$  square matrix with vanishing elements except the diagonal terms which are the corresponding elements of the column matrix  $(M-H)$ . In summation index form equation (29) can be written as

$$\left( \frac{\partial F}{\partial X} \right)_{jk} = - \sum_i (W^{-1})_{jk} \left[ \left( \frac{\partial H_i}{\partial X_j} \right) \left( \frac{\partial H_i}{\partial X_k} \right) + (M_i - H_i) \frac{\partial^2 H_i}{\partial X_k \partial X_j} \right] \quad (30)$$

Although comparison shows that the differential correction method of equation (25) can be obtained from the Newton-Raphson method of equations (28) and (29) by neglecting the second partial derivative terms in equation (29), the mathematical implication is not so simple and will be explored under method D.

### C. Generalized Newton-Raphson Method

The technique is an adaptation of an idea advanced by D. F. Davidenko<sup>[2]</sup> for solving a system of nonlinear equations. Convergence theorems and existence of solutions theorems will not be included in this paper.

Let  $G(X)$  be a vector function of a vector variable  $X$ , for which it is desired to find a value of  $X$  such that  $G(X)$  is zero. Assume  $X$  is a function of a scalar  $\lambda$  and define a new vector function

$$\phi(\lambda) = G[X(\lambda)] - (1-\lambda)G[X(0)] , \quad (31)$$

where  $X(0)$  is an arbitrary point. The function  $\phi(\lambda)$  satisfies the conditions  $\phi(0) = 0$  and  $\phi(1) = G[X(1)]$ . The function  $\phi(\lambda)$  is zero if and only if  $\frac{d\phi}{d\lambda}$  is zero. Differentiating equation (31) gives

$$\frac{d\phi}{d\lambda} = \frac{\partial G}{\partial X} \frac{dX}{d\lambda} + G[X(0)] . \quad (32)$$

The values of  $\frac{dX}{d\lambda}$  such that  $\frac{d\phi}{d\lambda}$  is zero describe an integral curve of the form

$$X(\lambda) = X(0) + \int_0^\lambda \frac{dX}{d\lambda} d\lambda , \quad (33)$$

such that  $G[X(\lambda)] - (1-\lambda)G[X(0)]$  is zero. The vector  $X(1)$  is a solution to the equation  $G(X) = 0$ . We apply this technique to the vector function  $F(X) = 0$  of equation (23). Substituting  $F(X)$  for  $G(X)$  in equation (32) and equating  $\frac{d\phi}{d\lambda}$  to zero gives

$$0 = \frac{\partial F}{\partial X} \frac{dX}{d\lambda} + F[X(0)] . \quad (34)$$

A unique solution for  $\frac{dX}{d\lambda}$  exists if  $\frac{\partial F}{\partial X}$  is non-singular. Thus

$$\frac{dX}{d\lambda} = -\left(\frac{\partial F}{\partial X}\right)^{-1} F[X(0)] , \quad (35)$$

and

$$X(1) = X(0) - \int_0^1 \left(\frac{\partial F}{\partial X}\right)^{-1} F[X(0)] d\lambda . \quad (36)$$

By using a first order integration technique, a recursive formula may be defined as

$$X_{i+1} = X_i - h \left(\frac{\partial F}{\partial X}\right)^{-1} F(X_i) . \quad (37)$$

Comparison of equations (28) and (37) shows that the Newton-Raphson method is a special case of equation (37) when the step-size variable  $h = 1$ .

The integration technique used in equation (36) is the variable step-size, fourth order Adam-Moulton predictor-corrector method. Since this technique is not self-starting, a fourth order Runge-Kutta process is used for starting values. Variable step-size integration technique enables the integration path to follow smoothly along the solution curve.

Both the Newton-Raphson and generalized Newton-Raphson method require evaluation of the Jacobian matrix  $\frac{\partial F}{\partial X}$  involving both the first and second partial derivatives of the function H as shown in equation (29). These evaluations are tedious, but possible, and are shown in Appendix I.

#### D. Generalized Differential Correction Method

Method C described in the previous section reduces the problem of solving for the zeros of a system of equations to that of integrating a set of first order differential equations. Application of the same technique to minimizing the quadratic form  $Q(X)$  of equation (22) directly is based on the condition that, for uncorrupted measurements, the quadratic form  $Q(X)$  is zero if and only if the vector  $[M-H(X)]$  is zero. Mathematically it implies that the absolute minimum of the quadratic function  $Q(X)$  is zero. The application to actual, or corrupted, measurements will be covered later.

To solve the vector equation  $[M-H(X)] = 0$ , we substitute  $[M-H(X)]$  for  $G(X)$  in equation (32) and equate  $\frac{d\phi}{d\lambda}$  to zero. The resulting equation is

$$0 = -\frac{\partial H}{\partial X} \frac{dX}{d\lambda} + [M-H(X(0))] \quad . \quad (38)$$

The matrix  $\frac{\partial H}{\partial X}$  is rectangular if the number of observations is greater than the number of parameters. It can be shown that there exists a unique solution to equation (38) if the rank of  $\frac{\partial H}{\partial X}$  is equal to the number of parameters. To solve for  $\frac{dX}{d\lambda}$ , we premultiply equation (38) by  $\left(\frac{\partial H}{\partial X}\right)^T$ . The matrix  $\left(\frac{\partial H}{\partial X}\right)^T \frac{\partial H}{\partial X}$  is non-singular, hence

$$\frac{dX}{d\lambda} = \left[ \left(\frac{\partial H}{\partial X}\right)^T \frac{\partial H}{\partial X} \right]^{-1} \left(\frac{\partial H}{\partial X}\right)^T [M-H(X(0))] . \quad (39)$$

The solution to  $Q(X) = 0$  is

$$X(1) = X(0) + \int_0^1 \left[ \left(\frac{\partial H}{\partial X}\right)^T \frac{\partial H}{\partial X} \right]^{-1} \left(\frac{\partial H}{\partial X}\right)^T [M-H(X(0))] d\lambda . \quad (40)$$

As before, a recursive formula may be defined by

$$X_{i+1} = X_i - h \left[ \left(\frac{\partial H}{\partial X}\right)^T \frac{\partial H}{\partial X} \right]^{-1} \left(\frac{\partial H}{\partial X}\right)^T [M-H(X_i)] . \quad (41)$$

If the step-size  $h$  is unity, the formula is the classical differential correction technique.

For any choice of initial estimate  $X_0$ , equation (40) converges to a minimum of  $Q(X)$  whether or not a solution to  $[M-H(X)] = 0$  exists. This can be explained by the integral solution curve defined by equation (33). The solution curve fails to exist when  $\frac{dX}{d\lambda} = 0$ . However,  $\frac{dX}{d\lambda} = 0$  implies  $\frac{\partial Q}{\partial X} = 0$ , which is necessary for a minimum.

In actual observations, measurements are always corrupted and the vector equation  $[M-H(X)]$  is nonvanishing at the absolute minimum. This corresponds to the fact that the absolute minimum of the quadratic function  $Q(X)$  for uncorrupted

measurements has been shifted and  $Q(X) = 0$  has no solution for corrupted measurements. However, equation (40) still can be used to search for a minimum of  $Q(X)$  by the argument in the previous paragraph.

The pattern by which the parameter  $X$  seeks the desired  $X$  depends on the sign of the function and the sign of its first derivative at an initial estimate  $X_0$ . Since both the Newton-Raphson method and generalized Newton-Raphson method search for zeros of  $F(X)$ , the desired  $X$  for which  $F(X) = 0$  will be tracked only if the initial estimate  $X_0$  is such that  $\left(\frac{\partial F}{\partial X}\right)^{-1}$  is non-singular between  $X_0$  and the desired  $X$ . On the other hand, the generalized differential correction method searches for a minimum of a positive definite function  $Q(X)$ . The desired  $X$  for which  $Q(X)$  is a minimum can be tracked if the initial estimate  $X_0$  is such that  $\left[\left(\frac{\partial H}{\partial X}\right)^T \frac{\partial H}{\partial X}\right]^{-1}$  is non-singular between  $X_0$  and the desired  $X$ , for which  $\frac{\partial Q}{\partial X} = 0$ .

Since  $F(X)$  is the first derivative of  $Q(X)$ , the independent variable distance between the neighboring extremes of  $Q(X)$  is in general wider than that between the  $F(X) = 0$  and a neighboring  $F(X)$  extreme, at least in a one-dimensional analogy. Accordingly, we infer that both the generalized and the classical differential correction methods can yield a convergence range of initial estimate  $X_0$  wider than both the Newton-Raphson and generalized Newton-Raphson methods. The variable step-size integration in the generalized differential correction method removes the constraint of linearization of the classical differential correction method, and therefore, the generalized differential correction method has a wider convergence range of initial estimate  $X_0$  than the classical differential correction method.



E. Other Methods

A recent survey of other numerical methods is given by Spang.<sup>[3]</sup> Since these methods are not suitable for the present application, they are not discussed here.

V. SIMULATION COMPARISONS

To simplify simulation processes without loss of generality we assume that observations are made at the center of the Earth at an infinite distance from the planet to avoid the corrections of observed data. In this way the theoretically computed values  $H$  can be used directly as observed data or can be used by introducing noise with normal distribution. The state-vector of a planetary satellite will be determined in case (i) for a stationary planet and case (ii) for a rotating planet by the four methods discussed herein. The principal aim of the simulation is to show that (1) the state-vector of a planetary artificial satellite can be accurately determined within a few days from the Earth-based Doppler data and (2) the generalized differential correction method can yield a convergence range of initial estimate  $X_0$  wider than the other methods.

A. Stationary Planet

This is the situation corresponding to the spectroscopic binary star case. Excluding the general singular situations (1) when  $e$  is zero,  $\omega$  and  $\tau$  are undefined and (2) when  $i$  is zero,  $\Omega$  is undefined, we note that the stationary planet case has two additional "intrinsic" singular situation. The first corresponds to the "infinite" degeneracy in the longitude of the ascending node  $\Omega$  for orbital planes of fixed inclination  $i$  and  $\pi - i$ . Observationally this means that any orbit with fixed  $a$ ,  $e$ ,  $\tau$ ,  $i$ ,  $\omega$ , and  $\mu$  but different  $\Omega$  will have the same

Doppler time history. Mathematically this observational degeneracy is indicated by the fact that when  $i' = 0$ ,  $\Omega$  drops out of equation (11). The first partial derivatives with respect to  $\Omega$  vanishes but the partial state-vector  $(a, e, \tau, i, \omega, \mu)$  still can be evaluated. The second singular case occurs when the inclination  $i$  is  $\frac{\pi}{2}$  or  $\frac{3\pi}{2}$ . Observationally there is no Doppler effect in this case and mathematically  $\frac{\partial H}{\partial i} = 0$  since  $\frac{\partial A}{\partial i} = 0$  as seen from Appendix I.

Without considering singular cases for simulation, the following set of parameters was arbitrarily chosen for testing and evaluating purposes:

$$a = 2788 \text{ km}$$

$$e = 0.289$$

$$\tau = 0 \text{ min}$$

$$i = 40^\circ$$

$$\omega = 283^\circ$$

$$\mu = 1.77 \times 10^7 \text{ km}^3/\text{min}^2$$

The above set of parameters is substituted in equation (11) to compute the theoretical radial range-rate  $H(X)$ . Observational data  $M$  are simulated by truncating the theoretical value  $H(X)$  to an appropriate number of significant figures corresponding to actual range-rate measurement accuracy. For the case shown herein, we arbitrarily truncated to three significant figures by dropping the fourth significant figure when it is less than five and adding one to the third significant figure when it is equal to or more than five. Noise pattern obtained this way may not approach the assumed normal distribution. A proper way of introducing noise in the theoretical data is to have a normally distributed noise generator incorporated in the programming. Since the actual range-rate measurement accuracy is

better than three significant figures, the deviations of the parameters from the true values are conservative. The results of the simulation are shown in Table I.

Initial computations using single precision on the Univac 1108 show that the results of iterative convergence processes differ for slightly different initial estimates, indicating problems in matrix inversion. When double precision is used throughout the computations, at least the first eight significant figures in the print-out show consistency and, therefore, accuracy in computations. All results shown are obtained by programming with double precision.

Table I is designed to show the initial estimate range within which the four above-mentioned methods can converge to the best estimate. It is seen that the generalized differential correction method has the widest range and the classical differential correction method the next. The Newton-Raphson and generalized Newton-Raphson methods have almost the same narrowest range. From the results shown and the fact that the generalized differential correction method requires much more computer time than the classical differential correction method (a ratio of about 10:1) we can conclude that for any given initial estimate  $X_0$  we should generally apply the classical differential correction method first. In case the classical method fails to converge, we can then apply the generalized differential correction method. If the generalized method also fails to converge, the initial estimate  $X_0$  has to be revised. Note in Table I that  $\frac{\partial F}{\partial X} = 0$  between  $a = 2677.0$  and  $a = 2677.8$ .

B. Moving Planet

In this case the degeneracy in observation is removed. For a slow moving planet the normal matrix may be ill-conditioned, but not singular, and the state-vector accuracy, especially in the parameter  $\Omega$ , increases as the number of orbits tracked increases.

In an attempt to estimate in a minimum number of orbits the state-vector of a satellite of a slowly moving distant planet, we realize that the near-degeneracy nature of the parameter  $\Omega$  is still a problem. For Mars during oppositions the relative angular displacement with respect to the Earth is less than one-half of a degree per day. The near-degeneracy is indicated by the fact that convergence does not take place until the initial estimates of the parameters other than  $\Omega$  are very close to the desired values. To circumvent the difficulty, we apply the observational data from the first orbit of the satellite of a slowly moving distant planet to the stationary planet case first and obtain an approximate partial state-vector ( $a, e, \tau, \omega, i$ ). Using the approximate partial state-vector thus obtained and any estimate of the parameter  $\Omega$ , we can quickly determine a new state-vector estimate including the parameter  $\Omega$ . If it is assumed that no systematic error is introduced in the measurements and noise is normally distributed, the accuracy of the complete state-vector estimate increases as (a) the number of orbits tracked increases, (b) the number of significant figures used in the simulated measurements increases, and (c) the data sample rate increases (to the extent that data are not correlated). The simulation results are shown in Table II.

Conservative one-sigma uncertainty for range-rate measurement is about  $10^{-4}$  m/sec. The theoretical maximum and minimum radial velocities of a planetary satellite of Mars with the following parameters are about  $9.039 \times 10^3$  km/hr and  $0.4228 \times 10^3$  km/hr, respectively, for data points separated by 0.9 hr:

$$a = 14,040 \text{ km}$$

$$e = 0.7$$

$$\tau = 2 \text{ hr}$$

$$i = 40^\circ$$

$$\omega = 30^\circ$$

$$\Omega = 50^\circ$$

$$\mu = 5.5637 \times 10^{11} \text{ km}^3/\text{hr}^2$$

The satellite period is about 14 hrs. To match the range-rate measurement accuracy for the case shown we can use the simulated observational data to 8 and 7 significant figures, respectively, for the maximum and minimum radial velocities. For a data sample rate other than once every 0.9 hr., the number of significant figures to be used for minimum radial velocity may be reduced if the minimum is very close to a zero crossing of the periodic Doppler shift curve.

Table II indicates that the state-vector of a planetary satellite can be determined to prescribed accuracy within a few days instead of a few months as described by Deutsch<sup>[4,5]</sup> in his adaptation of the spectroscopic binary star technique.

The fact that the parameter deviations drop off, but not smoothly, as the number of data points increases is an indication that the simulated noise introduced by rounding off processes does not have a normal distribution and may have a small bias.

Inspection of equation (11) shows that orbits with  $i$ ,  $\Omega$  and  $\pi - i$ ,  $\pi - \Omega$  are degenerate when  $\Omega' = 0$ . For planetary satellites  $\Omega'$  in general does not vanish and theoretically degeneracy should not be a problem.

#### VI. GENERAL STATISTICAL ESTIMATION CRITERION

For general cases of a rotating Earth at finite distance from a moving planet, equation (15) becomes

$$\dot{\underline{r}}_i \cdot (-\hat{\underline{z}}_i') = -\dot{\underline{D}}_i \cdot \hat{\underline{z}}_i' - \dot{\underline{R}}_i \cdot \hat{\underline{z}}_i' - (M_i) \hat{\underline{\rho}}_i \cdot \hat{\underline{z}}_i' - (\rho_i \dot{\theta}_{\rho_i}) \hat{\underline{\rho}}_{\perp i} \cdot \hat{\underline{z}}_i' \quad , \quad (42)$$

where  $M_i$  represents the only measured quantity of range-rate at  $t = t_i$ . The term  $(\rho_i \dot{\theta}_{\rho_i}) \hat{\underline{\rho}}_{\perp i} \cdot \hat{\underline{z}}_i'$  can be expressed as:

$$(\rho_i \dot{\theta}_{\rho_i}) \hat{\underline{\rho}}_{\perp i} \cdot \hat{\underline{z}}_i' = \dot{\underline{\rho}}_i \cdot \hat{\underline{z}}_i' - (\dot{\underline{\rho}}_i \cdot \hat{\underline{\rho}}_i) (\hat{\underline{\rho}}_i \cdot \hat{\underline{z}}_i') \quad . \quad (43)$$

The residual of equation (42) is:

$$\begin{aligned} \dot{\underline{r}}_i \cdot \hat{\underline{z}}_i' - \dot{\underline{D}}_i \cdot \hat{\underline{z}}_i' - \dot{\underline{R}}_i \cdot \hat{\underline{z}}_i' - (M_i) \hat{\underline{\rho}}_i \cdot \hat{\underline{z}}_i' - \dot{\underline{\rho}}_i \cdot \hat{\underline{z}}_i' \\ + (\dot{\underline{\rho}}_i \cdot \hat{\underline{\rho}}_i) (\hat{\underline{\rho}}_i \cdot \hat{\underline{z}}_i') = - (M_i - \dot{\underline{\rho}}_i \cdot \hat{\underline{\rho}}_i) (\hat{\underline{\rho}}_i \cdot \hat{\underline{z}}_i') \quad . \end{aligned} \quad (44)$$

The least square estimation criterion then is:

$$\begin{aligned} \sum_i (M_i - \dot{\underline{\rho}}_i \cdot \hat{\underline{\rho}}_i) (\hat{\underline{\rho}}_i \cdot \hat{\underline{z}}_i') \left[ (M_i - \dot{\underline{\rho}}_i \cdot \hat{\underline{\rho}}_i) \left( \frac{\partial \hat{\underline{\rho}}_i}{\partial X} \cdot \hat{\underline{z}}_i' \right) \right. \\ \left. - \left( \frac{\partial \dot{\underline{\rho}}_i}{\partial X} \cdot \hat{\underline{\rho}}_i + \dot{\underline{\rho}}_i \cdot \frac{\partial \hat{\underline{\rho}}_i}{\partial X} \right) (\hat{\underline{\rho}}_i \cdot \hat{\underline{z}}_i') \right] = 0 \quad , \quad (45) \end{aligned}$$

where

$$\frac{\partial \dot{\underline{p}}}{\partial \underline{X}} = \frac{\partial \dot{\underline{r}}}{\partial \underline{X}} \quad , \quad (46)$$

and

$$\frac{\partial \hat{\underline{p}}}{\partial \underline{X}} = \frac{1}{\rho} \frac{\partial \underline{r}}{\partial \underline{X}} - \hat{\underline{p}} \cdot \left( \frac{1}{\rho} \frac{\partial \underline{r}}{\partial \underline{X}} \right) \hat{\underline{p}} \quad . \quad (47)$$

It is seen that for general cases both  $\frac{\partial \dot{\underline{r}}}{\partial \underline{X}}$  and  $\frac{\partial \underline{r}}{\partial \underline{X}}$  are necessary in the state-vector estimation. The components of  $\frac{\partial \dot{\underline{r}}}{\partial \underline{X}}$  are shown in Appendix I and those of  $\frac{\partial \underline{r}}{\partial \underline{X}}$  are shown in Appendix II. Second partial derivatives with respect to  $\underline{r}$  have not been evaluated, since only the classical differential correction method and generalized differential correction method are used for general cases.

From equation (45) we note that the general least squares estimation criterion will be reduced to the conventional case if  $\hat{\underline{z}}'$  is taken to be  $\hat{\underline{p}}$  and use is made of the orthogonality relation between  $\frac{\partial \hat{\underline{p}}}{\partial \underline{X}}$  and  $\hat{\underline{p}}$ . Thus if  $\hat{\underline{z}}' = \hat{\underline{p}}$ , equation (45) becomes

$$\sum_i (M_i - \dot{\underline{p}}_i \cdot \hat{\underline{p}}_i) \left( \frac{\partial \dot{\underline{p}}_i}{\partial \underline{X}} \cdot \hat{\underline{p}}_i + \dot{\underline{p}}_i \cdot \frac{\partial \hat{\underline{p}}_i}{\partial \underline{X}} \right) = 0 \quad . \quad (48)$$

Simulation results for general cases using equation (45) as a criterion are in agreement with those shown in Tables I and II. This confirms the conclusion that in general the longitude of the ascending node of a planetary satellite can be determined to prescribed accuracy with a few days of Earth-based range-rate measurements.

Comparison of simulation results using equation (45) with those using equation (48) for the theoretical orbital elements and orbital orientation shown in Table II shows that differences are in the eighth significant figure. Although for the cases studied the state-vector estimates obtained by using equation (45) appear to be closer to the respective theoretical values than those obtained by using equation (48), it is inferred that the situation is highly dependent upon the choice of orbital elements and orbital orientation. Further study in this respect is desirable.

#### VII. PERTURBATIONS DUE TO AN OBLATE PLANET

The equatorial bulge of a planet causes the orbital plane of its satellite to regress, and the true orbit is no longer Keplerian with constant elements but osculating with varying elements. To take account of this perturbing effect the analysis presented above has to be modified by simple approximations.

Equation (1) and (2) hold true whether the orbit is Keplerian or osculating and

$$r = \frac{a(1-e^2)}{1+e \cos f} \quad (49)$$

remains correct in the osculating sense if we let  $a=a(t)$ ,  $e=e(t)$ , and  $f$  be defined by the Kepler's equation (13) with  $\tau=\tau(t)$ ,  $\Omega=\Omega(t)$ ,  $i=i(t)$ , and  $\omega=\omega(t)$ . It can be shown that equation (11) remains valid for an osculating orbit if the elements  $a, e, \tau, \Omega, i, \omega$  are in appropriate time-varying forms. General perturbations theory has shown that the oblateness effects of a central body on a satellite can be expressed by a time-varying state-vector of the satellite in terms of the spherical harmonic components of the gravitational potential of the central body. The perturbations can be grouped into (i) secular variations, (ii) long-period variations, and (iii) short-period variations. Kozai<sup>[6]</sup> has shown that for the first order secular perturbation the short-period variations in  $a, e$ , and  $i$  can be considered as time independent and



$$\begin{aligned}
 \Omega(t) &= \Omega_0 - \frac{3}{2} \frac{R_e^2}{a^2(1-e^2)^2} J_2 \bar{n}(\cos i)(t-t_0) = \Omega_0 - \dot{\Omega}(t-t_0) \\
 \omega(t) &= \omega_0 + \frac{3}{4} \frac{R_e^2}{a^2(1-e^2)^2} J_2 \bar{n}(4-5\sin^2 i)(t-t_0) \\
 &= \omega_0 + \dot{\omega}(t-t_0) \quad , \quad (50)
 \end{aligned}$$

$$m(t) = m_0 + \bar{n}(t-t_0) \quad , \quad \text{with } m_0 = \sqrt{\frac{\mu}{a^3}} (t_0 - \tau_0) \quad ,$$

where

$$\bar{n} = \sqrt{\frac{\mu}{a^3}} \left[ 1 + \frac{3}{4} \frac{R_e^2}{a^2(1-e^2)^2} J_2 (2-3\sin^2 i) \right] \quad ,$$

$J_2$  is the value of the second harmonic component of the central body potential,

$R_e$  is the equatorial radius of the central body, and

$\Omega_0, \omega_0$ , and  $m_0$  are the initial values (at  $t=t_0$ ) from which periodic perturbations have been removed.

Higher order secular variation terms and long-period variation terms involving higher order harmonic components  $J_3, J_4$  have been obtained by Brouwer<sup>[7]</sup>. Since equation (50) is referred to the planetary equatorial plane, a transformation of equation (11) to that plane at  $t = t_0$  is necessary to use equation (50). If we assume for mathematical simplicity that the "inertial" plane XY is the planetary equatorial plane, then equation (50) can be substituted directly into equations (11) and (13) for the state-vector evaluation as well as the  $J_2$  evaluation.

The exact evaluations of the partial derivatives are considerably complicated by the presence of the terms containing  $J_2$  together with  $a$ ,  $e$ ,  $i$ . For the classical differential correction and the Newton-Raphson methods, the iteration processes are not particularly sensitive to the partial derivatives and we suspect that the partial derivatives shown in Appendix I may be used to obtain the desired solution. For the generalized differential correction method exact evaluations are necessary, otherwise the integration process will not be able to follow the solution curve. If the parameter  $J_n$  is to be estimated, the evaluation of  $\frac{\partial H}{\partial J_n}$  is also necessary. To obtain simulation results involving the perturbation effects of an oblate planet also requires considerable revision of the existing computer program. Other perturbing forces due to the Sun and Earth can be incorporated in a similar fashion, when their effects on the satellite are expressed in appropriate time-varying form resembling equation (50).

#### VIII. CONCLUSIONS

The state-vector of a planetary artificial satellite is determined by using Earth-based range-rate measurements. The satellite velocity component in the direction from the planet-center to Earth-center instead of that from the satellite to an observation station is computed in a theoretical model. The relatively simple least squares estimation criterion thus obtained for the case of a planet at infinite distance facilitates the comparison study of numerical methods of solving a system of nonlinear equations.

Simulation results obtained by programming in double precision show that the longitude of the ascending node of a planetary satellite can be determined to prescribed accuracy within a few days of tracking.

The comparison study is made among (1) classical differential correction method, (2) Newton-Raphson method, (3) generalized differential correction method, and (4) generalized Newton-Raphson method. It indicates that the new generalized differential correction method has a convergence range of initial estimate wider than the other methods. The extension in the convergence range of initial estimate enhances the success of obtaining a preliminary state-vector in a short tracking period and is particularly important in planetary missions.

The effects of perturbations of non-central forces on the satellite can be incorporated in the formulation without resorting to numerical integration.

*C. C. H. Tang*  
C. C. H. Tang

*C. L. Greer*  
C. L. Greer

1014-<sup>CCHT</sup>  
CLG-jdc

Attachments  
Figures 1 and 2  
Tables I and II

BELLCOMM, INC.

REFERENCES

1. Smart, W. M., Spherical Astronomy, Chapter 14, Cambridge University Press, Cambridge (1936).
2. Davidenko, D. F., "Approximate Solution of Systems of Non-Linear Equations," Ukrainian Math Journal 5, 196-206, (1953).
3. Spang, H. A., "A Review of Minimization Techniques for Non-Linear Equations," SIAM Review, 4, 343-365, (1962).
4. Deutsch, A. J., "Orbits for Planetary Satellite from Doppler Data Alone," ARS Journal 30, 536-542, (1960).
5. Cohen, P. A. and Deutsch, A. J., "Error Analysis for Doppler Determined Satellite Orbits of Other Planets," ARS Journal 31, 1767-1768, (1961).
6. Kozai, Y., "The Motion of an Earth Satellite," Astronomical Journal 64, 367-377 (1959).
7. Brouwer, D., "Solution of the Problem of Artificial Satellite Theory Without Drag," Astronomical Journal 64, 378-397 (1959).

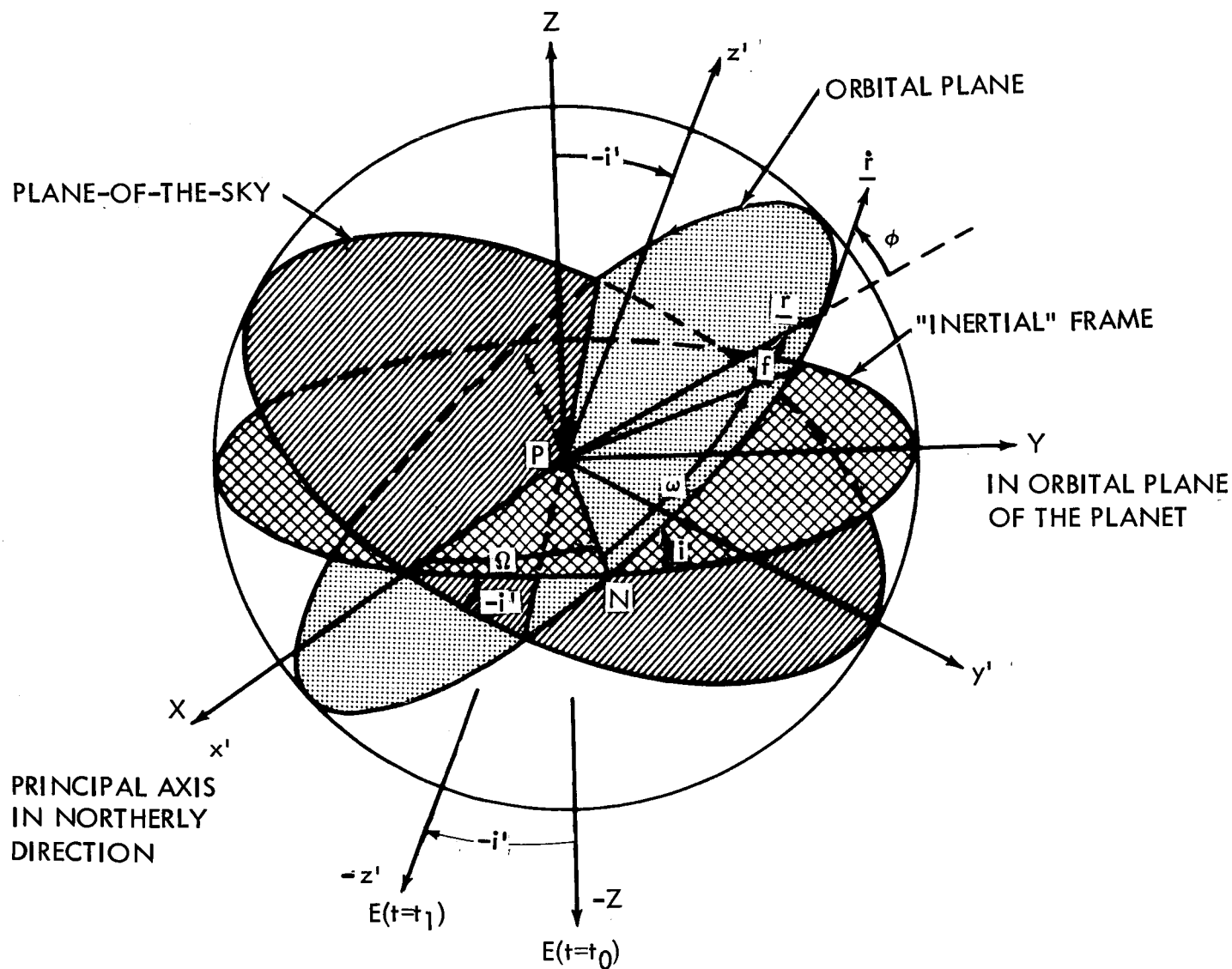


FIGURE 1 - PLANETOCENTRIC COORDINATE SYSTEMS



TABLE I SIMULATION RESULTS

PARAMETERS	THEORETICAL	ESTIMATED
$a$ (KM)	2788	2787.9892
$e$	0.289	0.28897788
$\tau$ (MIN)	0	-0.0076632791
$i$ (DEG)	40	40.000886
$\omega$ (DEG)	283	282.97972
$\mu$ (KM <sup>3</sup> /MIN <sup>2</sup> )	$1.77 \times 10^7$	
PERIOD (MIN)	219.853	

SAMPLING RATE: ONE EVERY FIVE MINUTES

SIMULATED MEASUREMENTS : OBTAINED BY ROUNDING OFF COMPUTED VALUES TO THREE SIGNIFICANT FIGURES.

$a$	$e$	$\tau$	$i$	$\omega$	$\mu$		C.D.C.	N.R.	G.N.R.	G.D.C.
2600.0	0.289	0	40	283	$1.77 \times 10^7$		C	X	X	C
2677.0	0.289	0	40	283	$1.77 \times 10^7$		C	X	X	C
* → 2677.8	0.289	0	40	283	$1.77 \times 10^7$		C	C	C	C
2900.0	0.289	0	40	283	$1.77 \times 10^7$		C	X	X	C
3300.0	0.289	0	40	283	$1.77 \times 10^7$		X	X	X	C
2788.0	0.100	0	40	283	$1.77 \times 10^7$		C	C	C	C
2788.0	0.230	0	40	283	$1.77 \times 10^7$		C	C	C	C
2788.0	0.250	0	40	283	$1.77 \times 10^7$		C	C	C	C
2788.0	0.500	0	40	283	$1.77 \times 10^7$		C	C	C	C
2788.0	0.289	0	20	283	$1.77 \times 10^7$		C	C	C	C
2788.0	0.289	0	30	283	$1.77 \times 10^7$		C	C	C	C
2788.0	0.289	0	60	283	$1.77 \times 10^7$		C	X	C	C
2788.0	0.289	0	40	240	$1.77 \times 10^7$		C	X	X	C
2788.0	0.289	0	40	260	$1.77 \times 10^7$		C	C	X	C
2788.0	0.289	0	40	300	$1.77 \times 10^7$		C	C	X	C
2788.0	0.289	0	40	320	$1.77 \times 10^7$		C	X	X	C
2000.0	0.500	10	40	270	$1.77 \times 10^7$		X	X	X	C
2500.0	0.250	-5	30	250	$1.77 \times 10^7$		C	X	X	C
3500.0	0.400	15	60	360	$1.77 \times 10^7$		X	X	X	C
4000.0	0.400	15	60	360	$1.77 \times 10^7$		X	X	X	C

## LEGEND

C: CONVERGE TO THE ESTIMATED PARAMETERS

X: FAIL TO CONVERGE OR CONVERGE TO WRONG SOLUTION.

$$* \rightarrow \frac{\partial F}{\partial X} = 0$$

C.D.C. : CLASSICAL DIFFERENTIAL CORRECTION METHOD

N.R. : NEWTON-RAPHSON METHOD

G.N.R. : GENERALIZED NEWTON-RAPHSON METHOD

G.D.C. : GENERALIZED DIFFERENTIAL CORRECTION METHOD

# TABLE II SIMULATION RESULTS

THEORETICAL PARAMETERS :  $\alpha = 14,040 \text{ KM.}$ ,  $e = 0.7$ ,  $\tau = 2 \text{ HR.}$ ,  $i = 40^\circ$ ,  $\omega = 30^\circ$ ,  $\Omega = 50^\circ$ ,  $\mu = 5.5637 \times 10^{11} \text{ KM}^3/\text{HR}^2$

PERIOD = 14.01357 HR  $\dot{i} = 0.4616^\circ/\text{DAY}$ .

S.P. <sup>+</sup>	S.F.*	DATA POINTS	$\alpha$	$e$	$\tau$	$i$	$\omega$	$\Omega$	$\mu$
.9 HR	3	25	14039.567	.70021562	2.0001692	39.985439	30.014237	62.979538	CONSTANT
		50	14040.020	.70010430	2.0000045	40.007584	29.990550	49.109398	
		100	14040.016	.70007512	1.999633	40.007477	29.988695	49.471878	
		150	14039.991	.70005345	2.000541	40.009189	29.989859	49.509018	
		200	14039.980	.70001423	2.0000961	40.005143	29.994315	49.785633	
		250	14040.006	.70002493	1.9999354	40.005259	29.993718	49.759198	
.9 HR	4	25	14040.088	.69998084	1.9999139	40.003033	29.997078	48.704795	CONSTANT
		50	14040.012	.70000085	1.9999667	40.001509	29.998951	49.846452	
		100	14040.007	.70000619	1.9999629	40.000917	29.998940	49.969658	
		150	14040.001	.70000620	1.9999844	40.000602	29.999229	49.996851	
		200	14040.000	.70000377	1.9999881	40.001033	29.998761	49.963483	
		250	14040.001	.70000188	1.9999853	40.000840	29.998987	49.973910	
		250	14041.024	.70000114	1.9999884	39.997444	29.999240	49.975526	5.5649170 10 <sup>11</sup>
.9 HR	7	25	14040.000	.70000002	2.0000000	39.999998	30.000003	50.000923	CONSTANT
		50	14040.000	.70000000	2.0000000	39.999998	30.000000	49.999915	
		100	14040.000	.70000000	2.0000000	39.999998	30.000000	50.000060	
		150	14040.000	.70000000	2.0000000	39.999998	30.000000	50.000001	
		200	14040.000	.70000000	2.0000000	39.999998	30.000000	49.999996	
		250	14040.000	.70000000	2.0000000	39.999998	30.000000	50.000022	
.2 HR									
.4 HR	3	100	14039.948	.70001929	2.0002088	39.995952	30.015607	51.344566	CONSTANT
.9 HR		25	14039.922	.70005740	2.0001212	39.987650	30.018057	53.877233	
			14039.567	.70021562	2.0001692	39.985439	30.014237	62.979538	

S.P.<sup>+</sup> : DATA SAMPLING PERIOD

S.F.\* : SIGNIFICANT FIGURES USED FOR SIMULATED MEASUREMENTS



# APPENDIX I

## Evaluations of the First and Second Partial Derivatives

$$H = - \left[ \frac{u}{a(1-e^2)} \right]^{\frac{1}{2}} \left\{ [\sin i \cos i' - \cos i \sin i' (\cos \Omega \cos \Omega' + \sin \Omega \sin \Omega')] [\cos(\omega+f) + e \cos \omega] + [(\sin \Omega \cos \Omega' - \cos \Omega \sin \Omega') \sin i'] [\sin(\omega+f) + e \sin \omega] \right\} .$$

$$\text{Let } H = K(AD_c + BF_s),$$

$$\text{where } K = - \left[ \frac{u}{a(1-e^2)} \right]^{\frac{1}{2}} .$$

$$D_c = C + e \cos \omega; \quad C = \cos(\omega+f).$$

$$F_s = S + e \sin \omega; \quad S = \sin(\omega+f).$$

$$A = \sin i \cos i' - \cos i \sin i' (\cos \Omega \cos \Omega' + \sin \Omega \sin \Omega').$$

$$B = (\sin \Omega \cos \Omega' - \cos \Omega \sin \Omega') \sin i'.$$

$$\frac{\partial H}{\partial a} = -\frac{H}{2a} - K(AS-BC) \frac{\partial f}{\partial a} .$$

$$\frac{\partial H}{\partial e} = \frac{eH}{1-e^2} - K[(AS-BC) \frac{\partial f}{\partial e} - A \cos \omega - B \sin \omega] .$$

$$\frac{\partial H}{\partial \mu} = \frac{H}{2\mu} - K(AS-BC) \frac{\partial f}{\partial \mu} .$$

$$\frac{\partial H}{\partial \tau} = -K(AS-BC) \frac{\partial f}{\partial \tau} .$$

$$\frac{\partial H}{\partial i} = K \frac{\partial A}{\partial i} D_c .$$

$$\frac{\partial H}{\partial \Omega} = K \left( \frac{\partial A}{\partial \Omega} D_c + \frac{\partial B}{\partial \Omega} F_s \right) .$$

$$\frac{\partial H}{\partial \omega} = -K(AF_s - BD_c) .$$

$$\frac{\partial f}{\partial a} = \frac{3}{2} \frac{K^3}{a\mu} (1+e \cos f)^2 (t-\tau) .$$

$$\frac{\partial f}{\partial e} = \frac{\sin f}{1-e^2} (2 + e \cos f) .$$

$$\frac{\partial f}{\partial \mu} = \frac{-K^3}{2\mu^2} (1 + e \cos f)^2 (t-\tau) .$$

$$\frac{\partial f}{\partial \tau} = \frac{K^3}{\mu} (1 + e \cos f)^2 .$$

$$\frac{\partial A}{\partial i} = \cos i \cos i' + (\cos \Omega \cos \Omega' + \sin \Omega \sin \Omega') \sin i \sin i' .$$

$$\frac{\partial A}{\partial \Omega} = (\sin \Omega \cos \Omega' - \cos \Omega \sin \Omega') \cos i \sin i' .$$

$$\frac{\partial B}{\partial \Omega} = (\cos \Omega \cos \Omega' + \sin \Omega \sin \Omega') \sin i'$$

$$\frac{\partial^2 H}{\partial a^2} = \frac{H}{2a^2} - \frac{1}{2a} \frac{\partial H}{\partial a} - K \left[ (AC+BS) \left( \frac{\partial f}{\partial a} \right)^2 - (AS-BC) \left( \frac{1}{2a} \frac{\partial f}{\partial a} - \frac{\partial^2 f}{\partial a^2} \right) \right].$$

$$\frac{\partial^2 H}{\partial e^2} = \frac{H}{(1-e^2)^2} + \frac{2e}{1-e^2} \frac{\partial H}{\partial e} - K \left[ (AC+BS) \left( \frac{\partial f}{\partial e} \right)^2 + (AS-BC) \frac{\partial^2 f}{\partial e^2} \right].$$

$$\frac{\partial^2 H}{\partial \mu^2} = \frac{1}{2\mu} \frac{\partial H}{\partial \mu} - \frac{H}{2\mu^2} - K \left[ (AC+BS) \left( \frac{\partial f}{\partial \mu} \right)^2 + (AS-BC) \left( \frac{1}{2\mu} \frac{\partial f}{\partial \mu} + \frac{\partial^2 f}{\partial \mu^2} \right) \right].$$

$$\frac{\partial^2 H}{\partial \tau^2} = -K \left[ (AC+BS) \left( \frac{\partial f}{\partial \tau} \right)^2 + (AS-BC) \left( \frac{\partial^2 f}{\partial \tau^2} \right) \right].$$

$$\frac{\partial^2 H}{\partial i^2} = K \frac{\partial^2 A}{\partial i^2} D_c = -K A D_c.$$

$$\frac{\partial^2 H}{\partial \omega^2} = -H.$$

$$\frac{\partial^2 H}{\partial \Omega^2} = K \left( \frac{\partial^2 A}{\partial \Omega^2} D_c - B F_s \right).$$

$$\frac{\partial^2 f}{\partial a^2} = - \left( \frac{5}{2a} + v \frac{\partial f}{\partial a} \right) \frac{\partial f}{\partial a}, \quad \text{where } v = \frac{2e \sin f}{1 + e \cos f}.$$

$$\frac{\partial^2 f}{\partial e^2} = \frac{1}{1-e^2} \left\{ \sin f \cos f + [2 \cos f (1+e \cos f) + e] \frac{\partial f}{\partial e} \right\}.$$

$$\frac{\partial^2 f}{\partial \mu^2} = - \left( \frac{1}{2\mu} + v \frac{\partial f}{\partial \mu} \right) \frac{\partial f}{\partial \mu}.$$

$$\frac{\partial^2 f}{\partial \tau^2} = -V \left( \frac{\partial f}{\partial \tau} \right)^2.$$

$$\frac{\partial^2 A}{\partial \Omega^2} = (\cos \Omega \cos \Omega' + \sin \Omega \sin \Omega') \cos i \sin i'.$$

$$\frac{\partial^2 H}{\partial a \partial e} = \frac{\partial^2 H}{\partial e \partial a} = -\frac{1}{2a} \frac{\partial H}{\partial e} - K \left[ (AC+BS) \frac{\partial f}{\partial a} \frac{\partial f}{\partial e} + (AS-BC) \left( \frac{e}{1-e^2} \frac{\partial f}{\partial a} + \frac{\partial^2 f}{\partial a \partial e} \right) \right].$$

$$\frac{\partial^2 H}{\partial a \partial \mu} = \frac{\partial^2 H}{\partial \mu \partial a} = -\frac{1}{2a} \frac{\partial H}{\partial \mu} - K \left[ (AC+BS) \frac{\partial f}{\partial a} \frac{\partial f}{\partial \mu} + (AS-BC) \left( \frac{1}{2\mu} \frac{\partial f}{\partial a} + \frac{\partial^2 f}{\partial a \partial \mu} \right) \right].$$

$$\frac{\partial^2 H}{\partial a \partial \tau} = \frac{\partial^2 H}{\partial \tau \partial a} = -\frac{1}{2a} \frac{\partial H}{\partial \tau} - K \left[ (AC+BS) \frac{\partial f}{\partial a} \frac{\partial f}{\partial \tau} + (AS-BC) \frac{\partial^2 f}{\partial a \partial \tau} \right].$$

$$\frac{\partial^2 H}{\partial a \partial i} = \frac{\partial^2 H}{\partial i \partial a} = -\frac{1}{2a} \frac{\partial H}{\partial i} - K S \frac{\partial A}{\partial i} \frac{\partial f}{\partial a}.$$

$$\frac{\partial^2 H}{\partial a \partial \omega} = \frac{\partial^2 H}{\partial \omega \partial a} = -\frac{1}{2a} \frac{\partial H}{\partial \omega} - K(AC+BS) \frac{\partial f}{\partial a}.$$

$$\frac{\partial^2 H}{\partial a \partial \Omega} = \frac{\partial^2 H}{\partial \Omega \partial a} = -\frac{1}{2a} \frac{\partial H}{\partial \Omega} - K \left( \frac{\partial A}{\partial \Omega} S - \frac{\partial B}{\partial \Omega} C \right) \frac{\partial f}{\partial a}.$$

$$\frac{\partial^2 H}{\partial e \partial \mu} = \frac{\partial^2 H}{\partial \mu \partial e} = \frac{1}{2\mu} \frac{\partial H}{\partial e} - K \left[ (AC+BS) \frac{\partial f}{\partial e} \frac{\partial f}{\partial \mu} + (AS-BC) \left( \frac{e}{1-e^2} \frac{\partial f}{\partial \mu} + \frac{\partial^2 f}{\partial e \partial \mu} \right) \right].$$

$$\frac{\partial^2 H}{\partial e \partial \tau} = \frac{\partial^2 H}{\partial \tau \partial e} = \frac{e}{1-e^2} \frac{\partial H}{\partial \tau} - K \left[ (AC+BS) \frac{\partial f}{\partial e} \frac{\partial f}{\partial \tau} + (AS-BC) \frac{\partial^2 f}{\partial e \partial \tau} \right].$$

$$\frac{\partial^2 H}{\partial e \partial i} = \frac{\partial^2 H}{\partial i \partial e} = \frac{e}{1-e^2} \frac{\partial H}{\partial i} + K \left[ \cos \omega - S \frac{\partial f}{\partial e} \right] \frac{\partial A}{\partial i}.$$

$$\frac{\partial^2 H}{\partial e \partial \omega} = \frac{\partial^2 H}{\partial \omega \partial e} = \frac{e}{1-e^2} \frac{\partial H}{\partial \omega} - K[(AC+BS) \frac{\partial f}{\partial e} + (A \sin \omega - B \cos \omega)] .$$

$$\frac{\partial^2 H}{\partial e \partial \Omega} = \frac{\partial^2 H}{\partial \Omega \partial e} = \frac{e}{1-e^2} \frac{\partial H}{\partial \Omega} - K \left[ \left( \frac{\partial A}{\partial \Omega} S - \frac{\partial B}{\partial \Omega} C \right) \frac{\partial f}{\partial e} - \left( \frac{\partial A}{\partial \Omega} \cos \omega + \frac{\partial B}{\partial \Omega} \sin \omega \right) \right] .$$

$$\frac{\partial^2 H}{\partial \mu \partial \tau} = \frac{\partial^2 H}{\partial \tau \partial \mu} = \frac{1}{2\mu} \frac{\partial H}{\partial \tau} - K[(AC+BS) \frac{\partial f}{\partial \mu} \frac{\partial f}{\partial \tau} + (AS-BC) \frac{\partial^2 f}{\partial \mu \partial \tau}] .$$

$$\frac{\partial^2 H}{\partial \mu \partial i} = \frac{\partial^2 H}{\partial i \partial \mu} = \frac{1}{2\mu} \frac{\partial H}{\partial i} - K S \frac{\partial A}{\partial i} \frac{\partial f}{\partial \mu} .$$

$$\frac{\partial^2 H}{\partial \mu \partial \omega} = \frac{\partial^2 H}{\partial \omega \partial \mu} = \frac{1}{2\mu} \frac{\partial H}{\partial \omega} - K(AC+BS) \frac{\partial f}{\partial \mu} .$$

$$\frac{\partial^2 H}{\partial \mu \partial \Omega} = \frac{\partial^2 H}{\partial \Omega \partial \mu} = \frac{1}{2\mu} \frac{\partial H}{\partial \Omega} - K \left( \frac{\partial A}{\partial \Omega} S - \frac{\partial B}{\partial \Omega} C \right) \frac{\partial f}{\partial \mu} .$$

$$\frac{\partial^2 H}{\partial \tau \partial i} = \frac{\partial^2 H}{\partial i \partial \tau} = -KS \frac{\partial A}{\partial i} \frac{\partial f}{\partial \tau} .$$

$$\frac{\partial^2 H}{\partial \tau \partial \omega} = \frac{\partial^2 H}{\partial \omega \partial \tau} = -K(AC+BS) \frac{\partial f}{\partial \tau} .$$

$$\frac{\partial^2 H}{\partial \tau \partial \Omega} = \frac{\partial^2 H}{\partial \Omega \partial \tau} = -K \left( \frac{\partial A}{\partial \Omega} S - \frac{\partial B}{\partial \Omega} C \right) \frac{\partial f}{\partial \tau} .$$

$$\frac{\partial^2 H}{\partial i \partial \omega} = \frac{\partial^2 H}{\partial \omega \partial i} = -KF_S \frac{\partial A}{\partial i} .$$

$$\frac{\partial^2 H}{\partial i \partial \Omega} = \frac{\partial^2 H}{\partial \Omega \partial i} = K D_c \frac{\partial^2 A}{\partial i \partial \Omega}.$$

$$\frac{\partial^2 H}{\partial \omega \partial \Omega} = \frac{\partial^2 H}{\partial \Omega \partial \omega} = -K \left( \frac{\partial A}{\partial \Omega} F_s - \frac{\partial B}{\partial \Omega} D_c \right).$$

$$\frac{\partial^2 f}{\partial a \partial e} = \frac{\partial^2 f}{\partial e \partial a} = \frac{1}{1-e^2} [2 \cos f (1 + e \cos f) - e] \frac{\partial f}{\partial a}.$$

$$\frac{\partial^2 f}{\partial a \partial \mu} = \frac{\partial^2 f}{\partial \mu \partial a} = - \left[ \frac{3}{2a} + v \frac{\partial f}{\partial a} \right] \frac{\partial f}{\partial \mu}.$$

$$\frac{\partial^2 f}{\partial a \partial \tau} = \frac{\partial^2 f}{\partial \tau \partial a} = - \left[ \frac{3}{2a} + v \frac{\partial f}{\partial a} \right] \frac{\partial f}{\partial \tau}.$$

$$\frac{\partial^2 f}{\partial e \partial \mu} = \frac{\partial^2 f}{\partial \mu \partial e} = \frac{1}{1-e^2} [2 \cos f (1+e \cos f) - e] \frac{\partial f}{\partial \mu}.$$

$$\frac{\partial^2 f}{\partial e \partial \tau} = \frac{\partial^2 f}{\partial \tau \partial e} = \frac{1}{1-e^2} [2 \cos f (1 + e \cos f) - e] \frac{\partial f}{\partial \tau}.$$

$$\frac{\partial^2 f}{\partial \mu \partial \tau} = \frac{\partial^2 f}{\partial \tau \partial \mu} = \left[ \frac{1}{2\mu} - v \frac{\partial f}{\partial \mu} \right] \frac{\partial f}{\partial \tau}.$$

$$\frac{\partial^2 A}{\partial i \partial \Omega} = (\cos \Omega \sin \Omega' - \sin \Omega \cos \Omega') \sin i \sin i'.$$

BELLCOMM, INC.

APPENDIX II

Evaluation of the First Partial Derivatives

$$h = \underline{r} \cdot (-\hat{\underline{z}}') = -\frac{a(1-e^2)}{1+e \cos f} \left\{ \left[ \sin i \cos i' - \cos i \sin i' \cos(\Omega-\Omega') \right] \sin(\omega+f) - \left[ \sin i' \sin(\Omega-\Omega') \right] \cos(\omega+f) \right\} .$$

Let

$$h = r(AS-BC),$$

where

$$r = -\frac{a(1-e^2)}{1+e \cos f},$$

and A, B, C, and S are defined in Appendix I.

$$\frac{\partial h}{\partial a} = \frac{h}{a} + L \frac{\partial f}{\partial a} ,$$

$$\frac{\partial h}{\partial e} = -h \left[ \frac{2e}{1-e^2} + \frac{\cos f}{1+e \cos f} \right] + L \frac{\partial f}{\partial e} ,$$

$$\frac{\partial h}{\partial \tau} = L \frac{\partial f}{\partial \tau} ,$$

$$\frac{\partial h}{\partial \mu} = L \frac{\partial f}{\partial \mu} ,$$

$$\frac{\partial h}{\partial \Omega} = r \left[ \frac{\partial A}{\partial \Omega} S - \frac{\partial B}{\partial \Omega} C \right] ,$$

## APPENDIX II

$$\frac{\partial h}{\partial i} = r \frac{\partial A}{\partial i} S ,$$

$$\frac{\partial h}{\partial \omega} = r(AC+BS) ,$$

where

$$L = h \frac{e \sin f}{1+e \cos f} + r(AC+BS).$$



BELLCOMM, INC.

DISTRIBUTION LIST

NASA Headquarters

Messrs. W. O. Armstrong/MTX  
P. E. Culbertson/MLA  
J. H. Disher/MLD  
F. P. Dixon/MTY  
R. W. Gillespie/MTE  
P. Grosz/MTL  
E. W. Hall/MTG  
D. P. Hearth/SL  
T. A. Keegan/MA-2  
D. R. Lord/MTD  
B. G. Noblitt/MTY  
S. C. Phillips/MA  
L. Reiffel/MA-6  
L. Roberts/OART-M (2)  
L. R. Scherer/MAL  
A. D. Schnyer/MTV  
F. J. Sullivan/RE  
M. G. Waugh/MTP  
J. W. Wild/MTE

NASA Headquarters Library

Manned Spacecraft Center

J. H. Boynton/FA4  
C. Covington/ET23  
D. E. Fielder/FA4  
E. H. Olling/ET4  
M. A. Silveira/EA2  
W. E. Stoney, Jr./ET  
J. M. West/AD

Marshall Space Flight Center

H. S. Becker/R-AS-DIR  
I. W. Carter/R-AS-V  
R. J. Harris/R-AS-VP  
F. L. Williams/R-AS-DIR

Kennedy Space Center

J. P. Claybourne/DE-FSO  
R. C. Hock/AA  
N. P. Salvail/DE-FSO

Goddard Space Flight Center

Messrs. F. O. Vonbun/550

Electronics Research Center

R. C. Duncan/S

Langley Research Center

W. R. Hook/60.300  
W. H. Michael/14.120  
C. H. Nelson/60.200

Ames Research Center

G. L. Smith/FST  
J. S. White/FST

Jet Propulsion Laboratory

W. G. Breckenridge/343  
T. W. Hamilton/312

Bellcomm, Inc.

F. G. Allen  
G. M. Anderson  
A. P. Boysen, Jr.  
J. O. Cappellari, Jr.  
D. A. Chisholm  
D. A. DeGraaf  
J. P. Downs  
R. E. Gradle  
D. R. Hagner  
V. Hamza  
P. L. Havenstein  
W. G. Heffron  
H. A. Helm  
J. J. Hibbert  
N. W. Hinnars  
B. T. Howard  
D. B. James  
J. Kranton  
D. D. Lloyd

BELLCOMM, INC.

DISTRIBUTION LIST (CONTINUED)

Bellcomm, Inc.

Messrs. K. E. Martersteck

R. K. McFarland

J. Z. Menard

G. T. Orrok

T. L. Powers

I. M. Ross

F. N. Schmidt

R. L. Selden

R. V. Sperry

C. M. Thomas

C. C. Tiffany

J. W. Timko

J. M. Tschirgi

J. E. Volonte

R. L. Wagner

J. E. Waldo

All members, Division 101

Department 1023

Library

Central Files

COPY TO